AD 727517

Security Classification

DOCUMENT CONTROL DATA - R & D

(Security classification of title, body of abstract and indexing annotation must be entered when the overall report is classified)

1. ORIGINATING ACTIVITY (Corporate author)

Aerospace Medical Research Laboratory,
Aerospace Division, Air Force Systems Command,
Wright-Patterson Air Force Base, Ohio 45433

2a. REPORT SECURITY CLASSIFICATION: UNCLASSIFIED

2b. GROUP: N/A

3. REPORT TITLE

MORPHOLOGY OF THE NON-DISEASED KIDNEY OF THE RHESUS MONKEY (MACACA MULATTA) WITH COMMENTS ON RENAL PHYSIOLOGY

4. DESCRIPTIVE NOTES (Type of report and inclusive dates)

5. AUTHOR(S) (First name, middle initial, last name)

C. Craig Tisher, M.D.

6. REPORT DATE	7a. TOTAL NO. OF PAGES	7b. NO. OF REFS
December 1970	43	24

8a. CONTRACT OR GRANT NO. F 33615-70-C- 1046

b. PROJECT NO. 6302

c.

d.

9a. ORIGINATOR'S REPORT NUMBER(S)

AMRL-TR-70-102

Paper No. 13

9b. OTHER REPORT NO(S) (Any other numbers that may be assigned this report)

10. DISTRIBUTION STATEMENT

Approved for public release; distribution unlimited

11. SUPPLEMENTARY NOTES

Conference was arranged by the Toxic Hazards Research Unit of SysteMed Corporation

12. SPONSORING MILITARY ACTIVITY

Aerospace Medical Research Laboratory, Aerospace Medical Div., Air Force Systems Command, W-PAFB, Ohio 45433

13. ABSTRACT

This paper was presented at the Proceedings of the 1st Annual Conference on Environmental Toxicology, sponsored by the SysteMed Corporation and held in Fairborn, Ohio on 9, 10, and 11 September 1970. Major technical areas discussed included toxicological evaluation of carbon monoxide, methodology, pathology, atmospheric contaminants, and toxicology of propellants and other military chemicals.

Key words:

Toxicology
Pathology

DD FORM 1 NOV 65 1473

40

AMRL-TR-70-102

PAPER NO. 13

MORPHOLOGY OF THE NON-DISEASED KIDNEY OF THE RHESUS MONKEY (MACACA MULATTA) WITH COMMENTS ON RENAL PHYSIOLOGY

C. Craig Tisher, M.D.

Duke University Medical Center
Durham, North Carolina

INTRODUCTION

The increased use of subhuman primates in biological research has made it mandatory for researchers to learn more about the morphology and physiology of these animals in non-diseased or steady states. The rhesus monkey (Macaca mulatta) represents a subhuman primate in which a wealth of such baseline biological information now available. The following paper addresses itself to the morphology of the kidney of this subhuman primate and, in addition, outlines certain parameters of renal function, particularly as they relate to the structure of the kidney. The discussion will include gross morphology as well as light and electron microscopic structural characteristics of the kidney. The material from which these observations were drawn consisted of young adult male and female rhesus monkeys weighing from 2.2 to 6.0 kg. A major goal of the light and electron microscopic studies was to determine the morphological alterations that result from the methods of procurement and preparation of percutaneous renal biopsies. Thus, in all animals used for ultrastructural studies, the renal tissue was prepared for electron microscopy by immersion fixation of percutaneous biopsies and by in vivo intravascular perfusion of the remaining intact kidney using several fixative and buffer combinations. Many of these observations are the subject of several recent publications (Tisher et al, 1969; Tisher and Rosen, 1967; Rosen and Tisher, 1968; Tisher et al, 1968; Tisher et al, 1970; Tisher et al, 1968; Tisher, in press) where the methods used in determining the status of renal function in individual animals and the method of tissue preservation employed for light and electron microscopic observations are described in detail.

RESULTS

The kidney of a young adult rhesus monkey weighing 3.0 kg weighs approximately 6.5 grams. The ratio of the body weight to the kidney weight in young adult animals is approximately 400:1. As shown in figure 1, the rhesus monkey kidney is unipapillate in structure. It is quite evident on examination of the gross specimen that the renal medulla of this animal is poorly developed, largely due to the virtual absence of an inner medullary zone. Figure 2 is a light micrograph detailing the appear-

ance of a sagittal section of kidney in which the plane of section passed through the mid-pelvic surface exactly parallel to and centered in the long axis of the papilla. The renal cortex is easily identified and its lower border, the juxtamedullary boundary, is indicated by a single arrow. The remainder of the sagittal section below the arrow represents medulla. In a recent study relating the morphology of the kidney to its concentrating ability (Tisher, in press) it was found that in 21 kidneys obtained from 13 animals, 56% of the entire thickness of the sagittal section represented medulla. However, the inner medullary zone accounted for only 14% of the entire sagittal surface. Thus, the very abbreviated renal medulla of this animal is largely due to the absence of a well-developed inner medullary zone. Urinary concentration studies performed in our laboratory reveal that after 24 to 45 hours of complete fluid deprivation these animals can maximally concentrate their urine to 1412 ± 151 mOsm/kg H_2O (range 1126 to 1670 mOsm/kg H_2O) (Tisher, in press). This compares quite favorably to man who can concentrate maximally to 1000 ± 200 mOsm/kg H_2O and possesses a kidney with a well developed inner medulla with long loops of Henle. This finding is of physiological significance since it has long been accepted that in mammals the ability to concentrate urine maximally is directly related to the length of the renal medulla and to the long loops of Henle (Berliner and Bennett, 1967). In short, the rhesus monkey represents a striking exception to this generally accepted rule. A more detailed discussion of this problem can be found in articles by Tisher et al, 1968; Tisher et al, 1970; and Tisher, in press.

Before beginning a presentation of the morphology of the individual components of the nephron, it should be noted that the term renal corpuscle rather than the term glomerulus will be used to designate that portion of the nephron which includes: 1) the capillary network lined by endothelial cells; 2) a central region of mesangial cells with continuous mesangial matrix material; and 3) visceral and parietal epithelial cells and their associated basement membranes. The basic structure of the renal corpuscle of the rhesus monkey kidney is similar to that of other laboratory animals and man. It is composed of the four basic cell types which include the endothelial cells that line the glomerular capillaries, the central stalk or mesangial cells, the visceral epithelial cells with their foot processes that come into contact with the external surface of the basement membrane of the peripheral capillary loops and the parietal epithelial cells that line Bowman's capsule. Figure 3 is a light micrograph denoting the relative position of these four cell types in the renal corpuscle of the rhesus monkey kidney, and figure 4 is an electron micrograph demonstrating the same features at higher resolution.

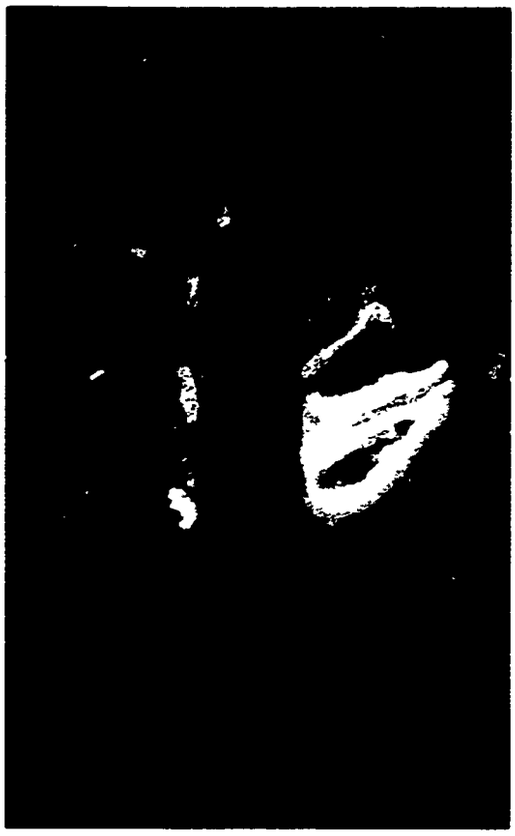

Figure 1. GROSS APPEARANCE OF THE CUT SURFACE OF A BIVALVED KIDNEY FROM A 3.4 KG RHESUS MONKEY. The boundary between the cortex and medulla is easily discernible. The papilla is blunted and opens into a simple type renal pelvis.

Figure 2. LOW POWER LIGHT MICROGRAPH SHOWING THE SAGITTAL SURFACE OF A BIVALVED RHESUS MONKEY KIDNEY. A single arrow denotes the cortico-medullary boundary at the level of the arcuate vessels. Gomori trichrome stain. X 4.2

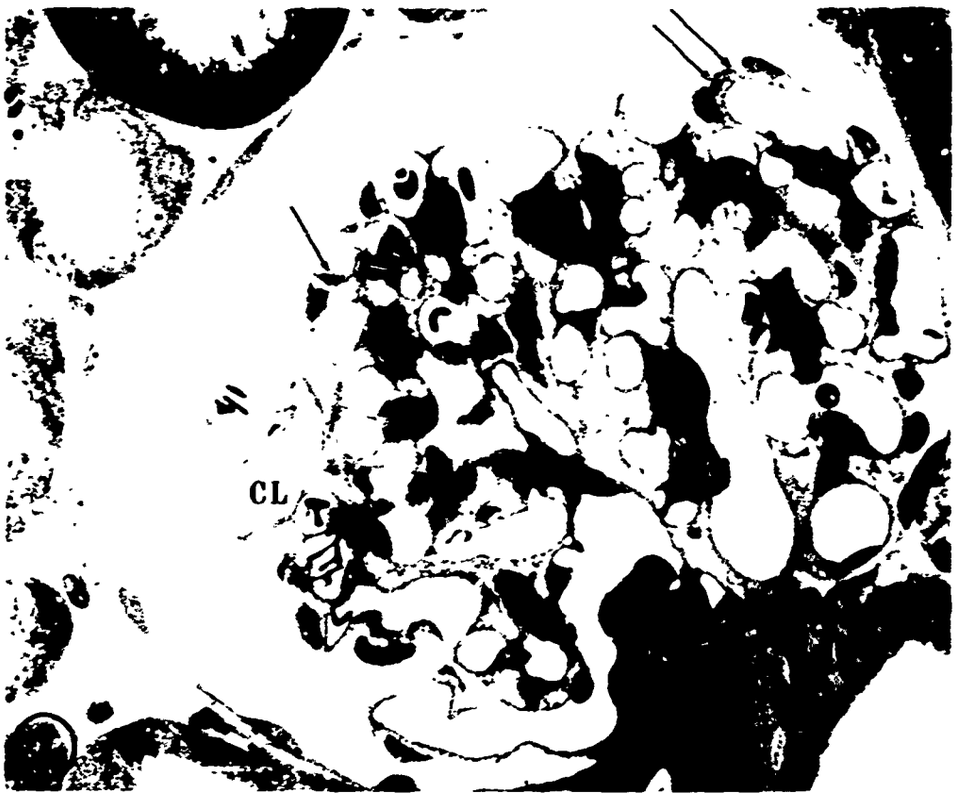

Figure 3. PHOTOMICROGRAPH OF A RENAL CORPUSCLE FROM A NON-DISEASED RHESUS MONKEY. The capillary lumens (CL) are patent and contain red blood cells. The mesangial cells (Me) are dark staining while the endothelial cells (arrow) and visceral epithelial cells (double arrow) are more pale staining. X 730

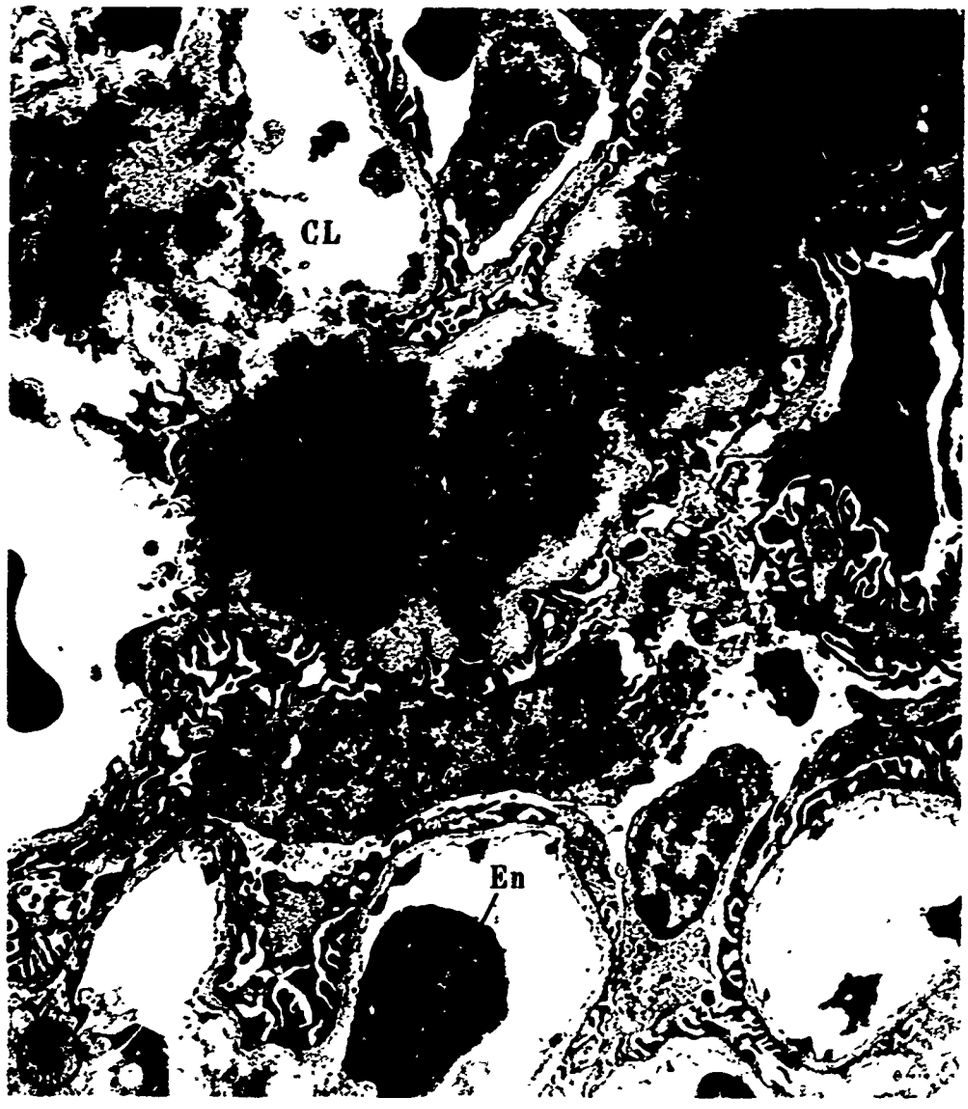

Figure 4. ELECTRON MICROGRAPH SHOWING PART OF A GLOMERULAR TUFT WITH CHARACTERISTIC MESANGIAL CELLS (Me), VISCERAL EPITHELIAL CELLS (VE), AND ENDOTHELIAL CELLS (En). CL, capillary lumen. X 4, 700

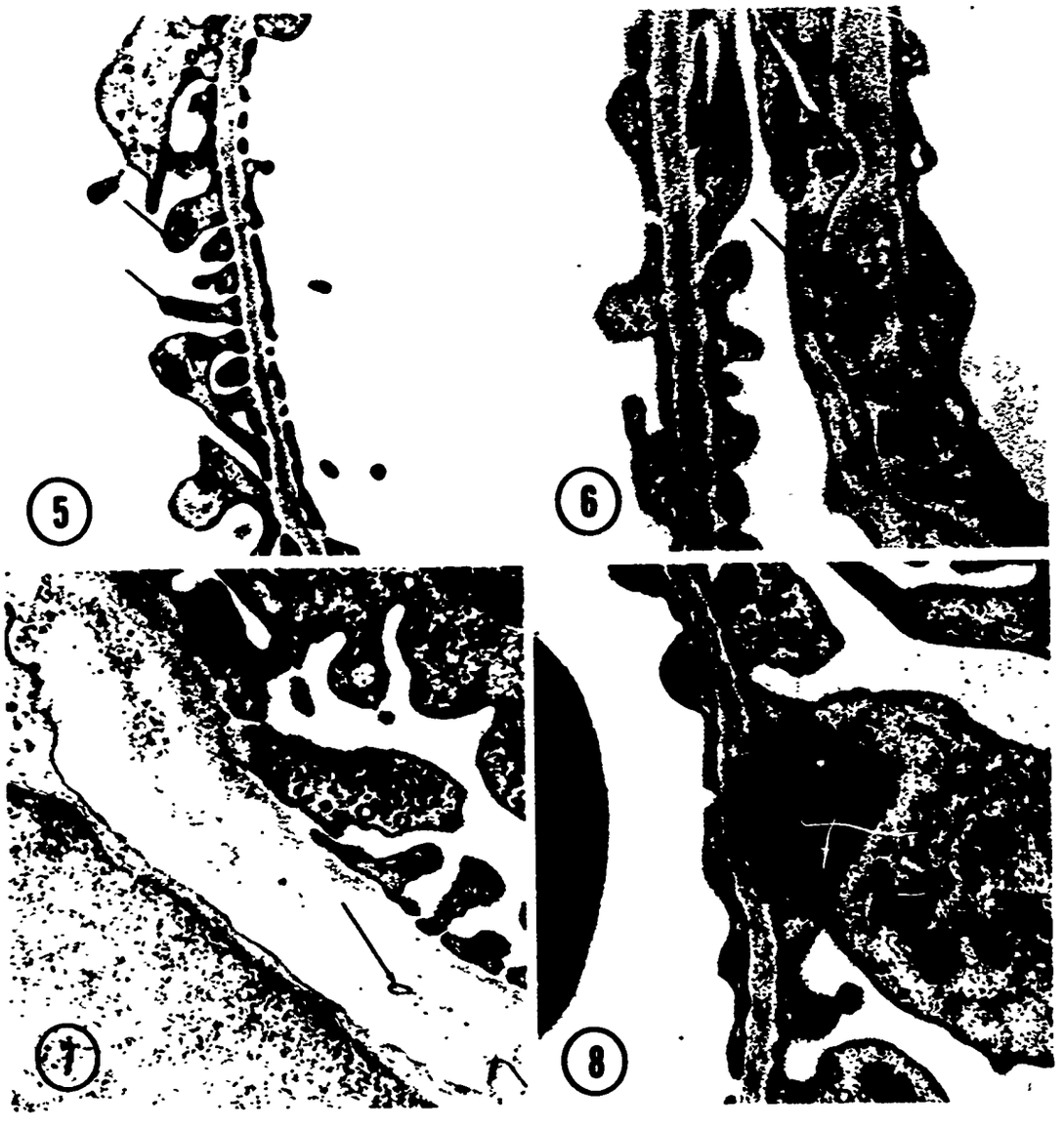
5
6
7
8

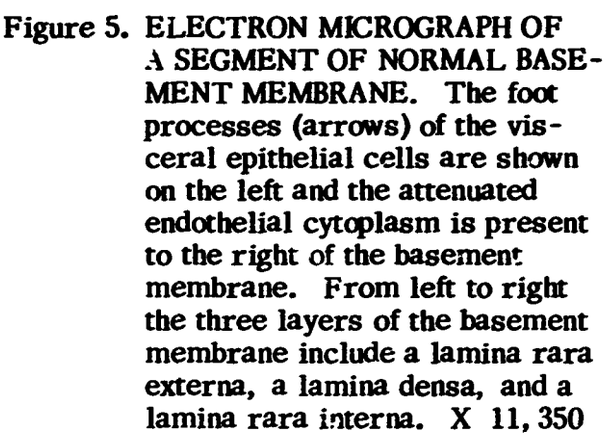

Figure 5. ELECTRON MICROGRAPH OF A SEGMENT OF NORMAL BASEMENT MEMBRANE. The foot processes (arrows) of the visceral epithelial cells are shown on the left and the attenuated endothelial cytoplasm is present to the right of the basement membrane. From left to right the three layers of the basement membrane include a lamina rara externa, a lamina densa, and a lamina rara interna. X 11,350

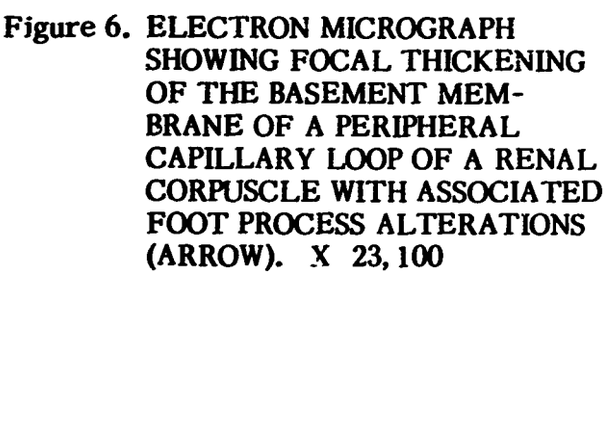

Figure 6. ELECTRON MICROGRAPH SHOWING FOCAL THICKENING OF THE BASEMENT MEMBRANE OF A PERIPHERAL CAPILLARY LOOP OF A RENAL CORPUSCLE WITH ASSOCIATED FOOT PROCESS ALTERATIONS (ARROW). X 23,100

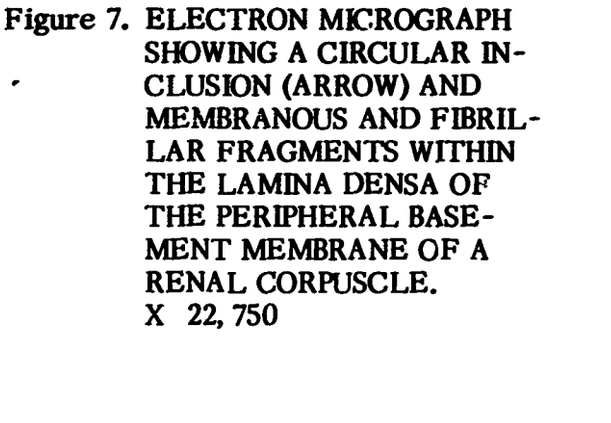

Figure 7. ELECTRON MICROGRAPH SHOWING A CIRCULAR INCLUSION (ARROW) AND MEMBRANOUS AND FIBRILLAR FRAGMENTS WITHIN THE LAMINA DENSA OF THE PERIPHERAL BASEMENT MEMBRANE OF A RENAL CORPUSCLE.
X 22,750

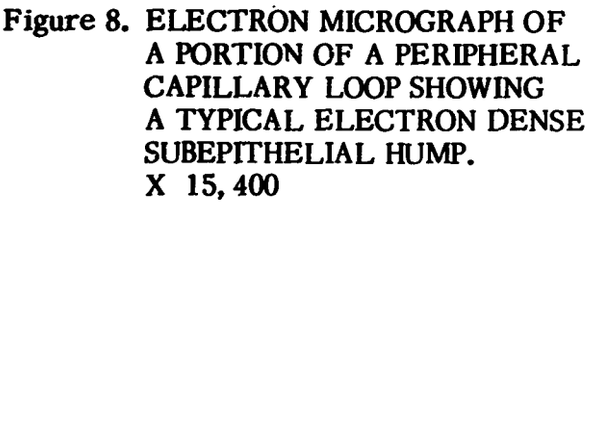

Figure 8. ELECTRON MICROGRAPH OF A PORTION OF A PERIPHERAL CAPILLARY LOOP SHOWING A TYPICAL ELECTRON DENSE SUBEPITHELIAL HUMP.
X 15,400

Because the basic ultrastructure of the renal corpuscle of the rhesus monkey kidney is similar to that of mouse, rat and man (Rosen and Tisher, 1968) a detailed description will not be offered here. A few features of significance will be discussed, however. As in other animals the basement membrane of the peripheral capillary loops is composed of a central lamina densa and two peripheral electron lucent layers, a lamina rara externa and interna (figure 5). Each of the latter two layers comprises about one tenth of the total membrane thickness. The basement membrane has been found to be fairly uniform in thickness measuring approximately 1840 ± 290 angstroms (standard deviation, N = 150) (Rosen and Tisher, 1968). This thickness is considerably less than that of the human which has been found to be approximately 3288 angstroms (Jorgensen and Bentzon, 1968). Focal thickening of the basement membrane is occasionally observed. This is sometimes associated with localized alterations of the foot processes overlying the involved area (figure 6). Not infrequently small dense deposits and circular inclusions are observed in the lamina densa and occasionally in the lamina rara externa (figure 7). These usually measure 500-1800 angstroms in diameter, are at times membrane-limited, and are also related to focal foot process alterations. Infrequently, large hump-shaped subepithelial densities are observed, not unlike those reported in the renal corpuscles of patients with poststreptococcal glomerulonephritis (Strunk et al, 1964) or those induced by chronic injections of foreign protein (figure 8). It is possible that such deposits could reflect the handling of foreign protein that has entered the circulation such as that associated with extensive testing for tuberculosis, a common procedure these animals have undergone. Whatever the etiology of these densities, their presence in nondiseased animals serves to illustrate the difficulty and pitfalls that occur in identification of glomerular disease processes with the aid of the electron microscope.

Certain variations are observed within the cellular components of the rhesus monkey renal corpuscle which deserve additional emphasis. Crystalline structures measuring 0.2 to 0.7 microns are found within endothelial cells (Rosen and Tisher, 1968; De Martino et al, 1969). They are composed of a lattice network formed by 250 to 300 angstrom circular or possibly hexagonal elements that interconnect with each other (figure 9). Similar structures are also present in the endothelial cells of peritubular capillaries (figure 10). The inclusions are usually in intimate contact with the endoplasmic reticulum. They have also been described in the endothelium of pulmonary and hepatic capillaries of rhesus monkeys (De Martino et al, 1969). Similar structures have been reported in the endothelium lining capillaries within the lamina propria of the ileum and transverse colon of the cynos monkey (Macaca irus) (Kanamitsu et al, 1967) and within monkey kidney cell cultures infected with rubella virus (Kim and Boatman, 1967). It is not clear what the significance of these endothelial crystalline inclusions is. It does not seem likely that this is a secretion product. The possibility that this structure represents some type of viral inclusion within the endothelial cell cannot be excluded at this time.

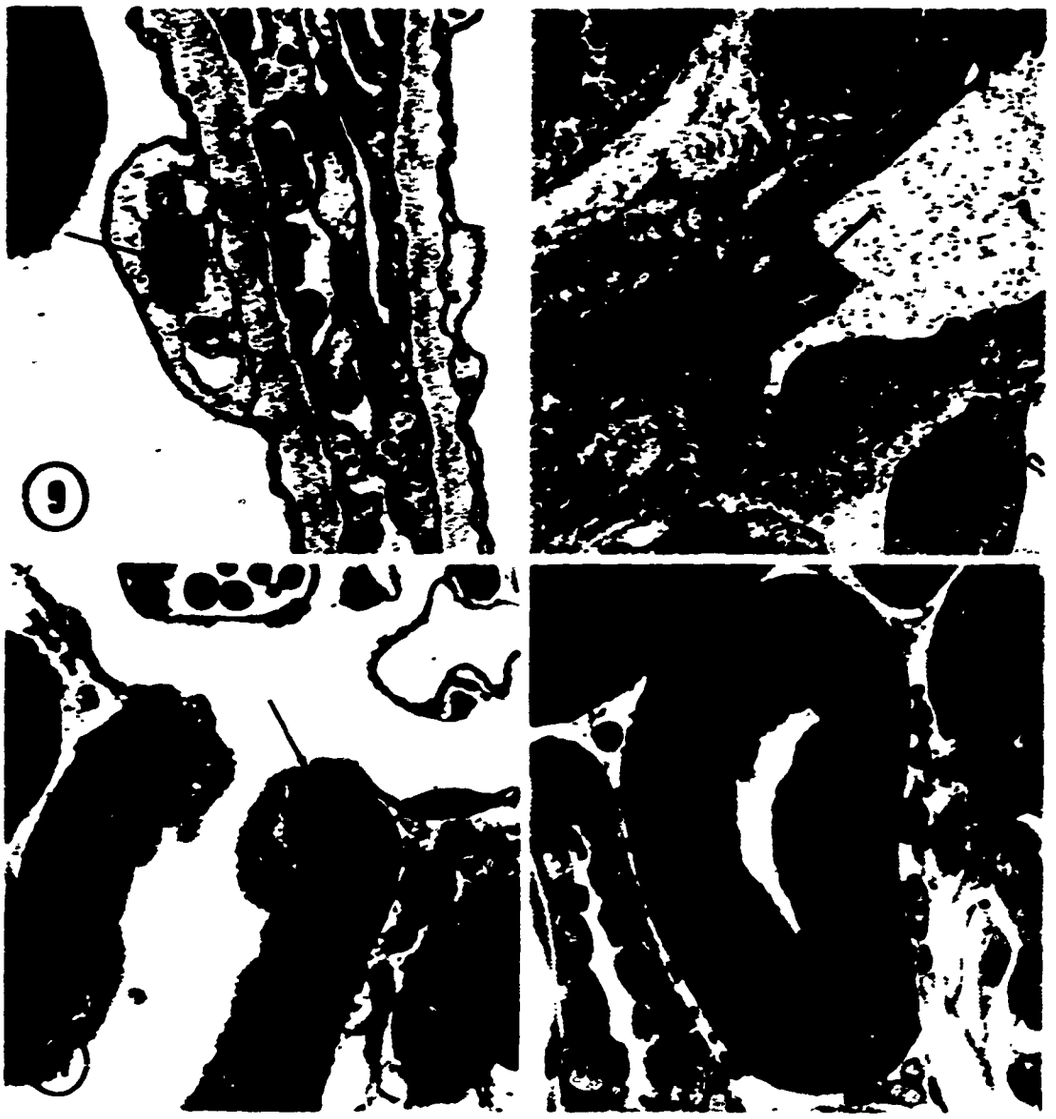

Figure 9. ELECTRON MICROGRAPH DEMONSTRATING A CRYSTALLINE INCLUSION (ARROW) WITHIN A GLOMERULAR ENDOTHELIAL CELL. X 21,600

Figure 10. CRYSTALLINE INCLUSION (ARROW) IN AN ENDOTHELIAL CELL OF A PERITUBULAR CAPILLARY WHICH IS IDENTICAL IN APPEARANCE TO THAT WITHIN THE ENDOTHELIUM LINING GLOMERULAR CAPILLARIES. (See figure 9 for comparison). X 12,300

Figure 11. PHOTOMICROGRAPH DEPICTING THE ABRUPT TRANSITION (ARROW) FROM LOW LYING SQUAMOUS EPITHELIUM LINING BOWMAN'S CAPSULE TO TALL COLUMNAR EPITHELIUM CHARACTERISTIC OF THE FIRST SEGMENT OF THE PROXIMAL TUBULE. X 500

Figure 12. PHOTOMICROGRAPH OF THE FIRST SEGMENT OF THE PROXIMAL TUBULE. The epithelium is tall and columnar, the brush border is well developed, and the cells are packed with elongate mitochondria. X 700

In the proximal tubule of the rhesus monkey, three distinct segments are identifiable by both light and electron microscopy. The segments can be defined by the morphology of their individual cellular components and by their relationship to other regions of the nephron. The first segment, which in general corresponds to the pars convoluta of the proximal tubule begins as an abrupt transition from the flattened squamous epithelial cells lining Bowman's capsule (figure 11). The cells are tall columnar and exhibit a well-developed PAS positive brush border and numerous elongate mitochondrial profiles (figure 12). Cells of the middle or second segment of the proximal tubule are low columnar in shape and possess a shorter and often more irregular brush border than those of the first segment (figure 13). Mitochondria are generally more tortuous and seldom elongate. Lipid droplets are most commonly observed in the second segment and situated along the base of the cell. The third segment of the proximal tubule corresponds in general to the pars recta or pars descendens. The cells of this segment are cuboidal in shape, exhibit a convex luminal surface and are covered by a distinct brush border. These cells contain far fewer organelles than cells of the first two segments of the proximal tubule and are generally less complex in structure (figure 14). The transition from the terminal proximal tubule to the thin descending limb of Henle is generally gradual and marked by the accumulation of large deposits of lipofuscin or degeneration pigment (figure 15).

Figures 16 through 19 represent electron micrographs of the neck region and the three segments of the proximal tubule. Since the fine structure of these cells does not vary greatly from that observed in the human kidney and in other laboratory animals, a detailed discussion will not be presented here. See reference 21 for further descriptions. The general cell shape, size, and configuration of the proximal tubule cells is nearly identical in man and rhesus monkey. One difference, however, is the presence of occasional distinct outpouching or evaginations at the base of proximal tubule cells in the monkey (figure 20). These structures are present in the first two segments of the tubule and are often associated with bands of coarse fibrils which extend across the mouth or neck of these evaginations. Similar structures have been observed in the proximal tubule of the rat (Strunk, 1964). Their structural and functional significance, if any, is unknown.

The microbody is the most common single membrane-limited inclusion body (SMLIB) in the rhesus monkey proximal tubule (Tisher et al, 1969), whereas cytosomes are the most common SMLIB present within the proximal tubule of the human kidney (Svoboda and Higginson, 1964). The structure of the microbody in the monkey is considerably different from that of man. In addition, a considerable variation in the appearance of microbodies in the monkey kidney is evident, depending upon the type of fixation that is employed. When tissue is preserved by in vivo intravascular perfusion of fixative, the microbodies are elongate in structure and possess one or more marginal plates along their outer limiting membrane (figure 21). When the tissue is preserved by immersion fixation, the marginal plates are often broken or fractured resulting in grotesquely angulated structural configurations (figures 22 and 23). See references 20 and 21 for a more detailed discussion. The renal microbodies in the human are usually spherical in structure with less prominent marginal plates (Tisher et al, 1966). It should be emphasized that thus far microbodies have only been found in the proximal tubule of the mammalian nephron.

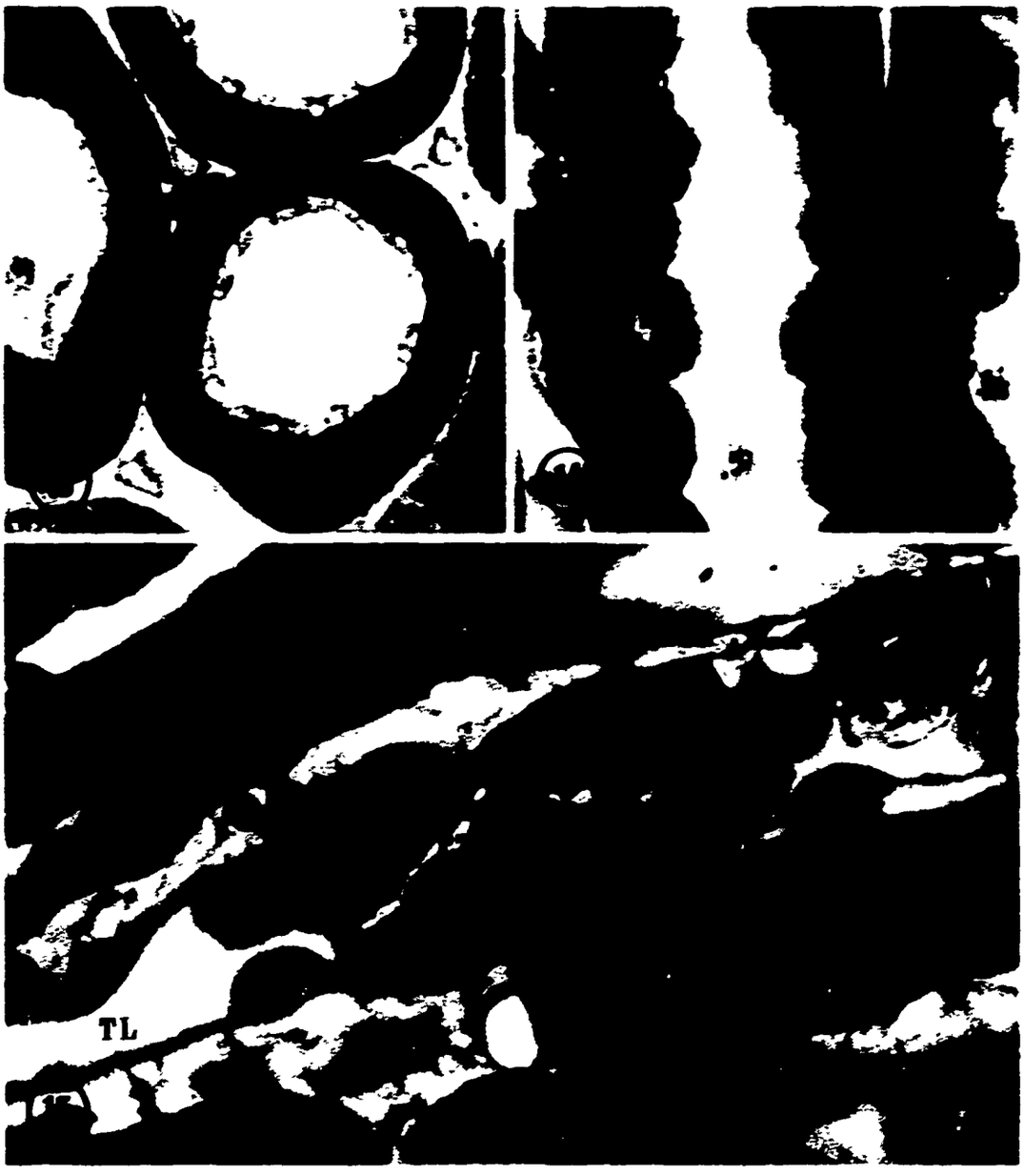

Figure 13. PHOTOMICROGRAPH OF THREE ADJACENT TUBULES CHARACTERISTIC OF THE SECOND SEGMENT OF THE PROXIMAL TUBULE. X 800

Figure 14. PHOTOMICROGRAPH CHARACTERISTIC OF THE THIRD SEGMENT OF THE PROXIMAL TUBULE. Cells are cuboidal in shape and have a convex luminal border. X 800

Figure 15. PHOTOMICROGRAPH SHOWING THE CHARACTERISTIC GRADUAL TRANSITION FROM THE TERMINAL PROXIMAL TUBULE (PT) ON THE RIGHT TO THE EARLY DESCENDING THIN LIMB (TL) OF HENLE'S LOOP ON THE LEFT. X 890

Figure 16. ELECTRON MICROGRAPH DEMONSTRATING TRANSITION FROM SQUAMOUS EPITHELIUM (ARROW) LINING BOWMAN'S CAPSULE TO THE COLUMNAR CELLS OF THE PROXIMAL TUBULE ABOVE. BS, Bowman's space; BM, basement membrane; RBC, red blood cell; VE, visceral epithelial cell. X 9250


PC

Figure 17. ELECTRON MICROGRAPH OF A TALL COLUMNAR CELL FROM THE FIRST SEGMENT OF THE PROXIMAL TUBULE. Elongate mitochondrial profiles (M) are enclosed in plications of the basal plasmalemma. The apical system of vesicles, vacuoles and dense tubules is well-developed. PC, peritubular capillary; AV, apical vacuole. X 10,000

Figure 18. ELECTRON MICROGRAPH OF A PROXIMAL TUBULE CELL FROM THE SECOND SEGMENT. The brush border (BB) is more irregular than that of the first segment and occasional skip areas (arrow) are noted. Apical vesicles and dense tubules are not as extensively developed but apical vacuoles (AV) are often more prominent. The cell is low columnar and lateral interdigitations with adjacent cells are less complex when compared to the first segment. C, cytosome. X 13,175

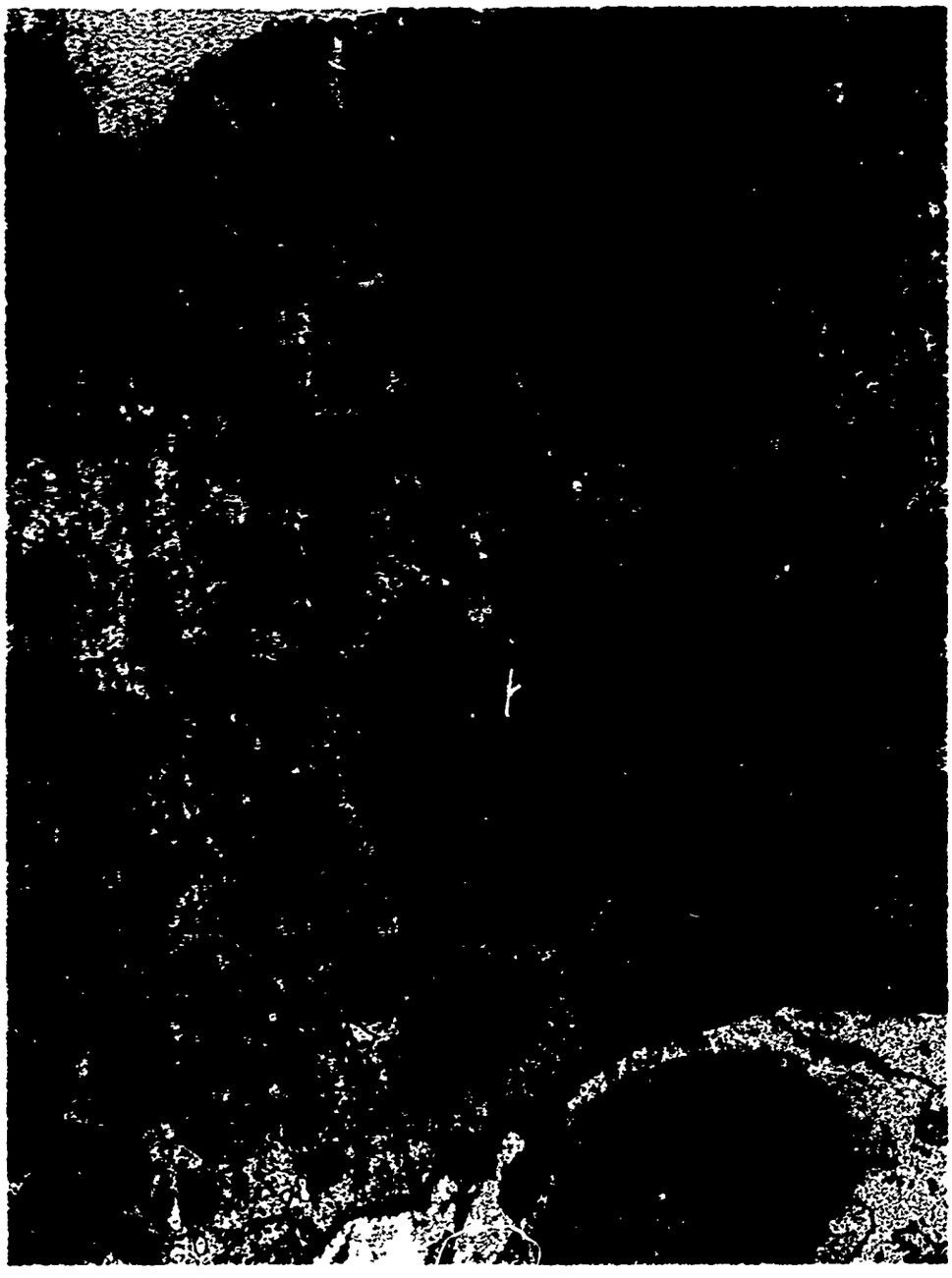

Figure 19. ELECTRON MICROGRAPH SHOWING A PROXIMAL TUBULE CELL CHARACTERISTIC OF THE THIRD SEGMENT. The cells are cuboidal and exhibit a well-developed brush border. Apical dense tubules and apical vacuoles are not extensive in this segment, although small apical vesicles are abundant. Microbodies (Mb) are the most common SMLIB in this segment. Note the relatively thin basement membrane (arrow). IC, interstitial cell. X 10,500

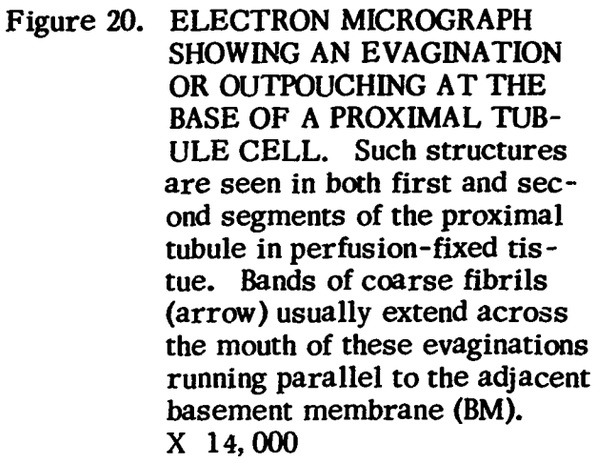

Figure 20. ELECTRON MICROGRAPH SHOWING AN EVAGINATION OR OUTPOUCHING AT THE BASE OF A PROXIMAL TUBULE CELL. Such structures are seen in both first and second segments of the proximal tubule in perfusion-fixed tistue. Bands of coarse fibrils (arrow) usually extend across the mouth of these evaginations running parallel to the adjacent basement membrane (BM). X 14,000

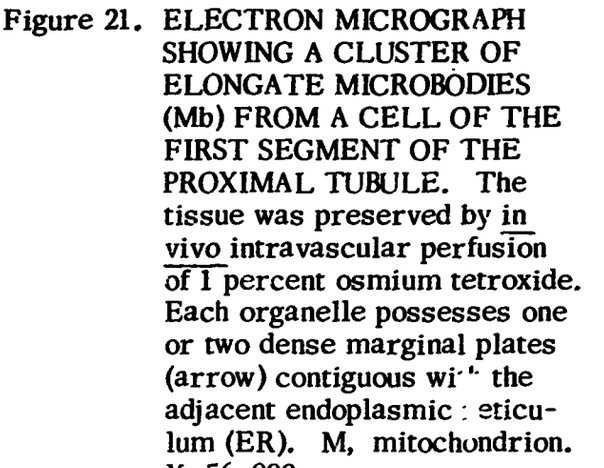

Figure 21. ELECTRON MICROGRAPH SHOWING A CLUSTER OF ELONGATE MICROBODIES (Mb) FROM A CELL OF THE FIRST SEGMENT OF THE PROXIMAL TUBULE. The tissue was preserved by in vivo intravascular perfusion of 1 percent osmium tetroxide. Each organelle possesses one or two dense marginal plates (arrow) contiguous wi" the adjacent endoplasmic : eticulum (ER). M, mitochondrion. X 56,000

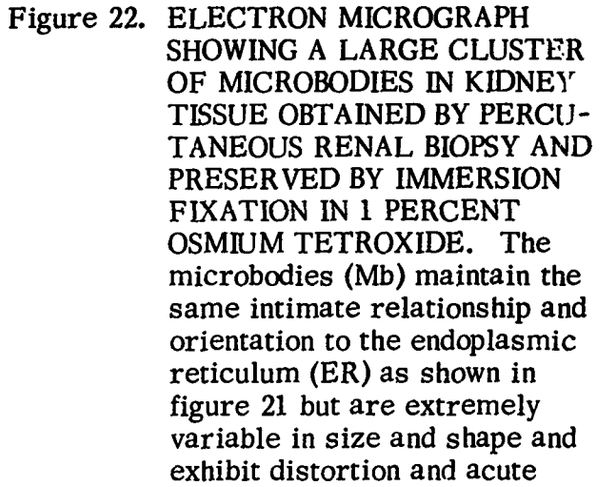

Figure 22. ELECTRON MICROGRAPH SHOWING A LARGE CLUSTER OF MICROBODIES IN KIDNEY TISSUE OBTAINED BY PERCUTANEOUS RENAL BIOPSY AND PRESERVED BY IMMERSION FIXATION IN 1 PERCENT OSMIUM TETROXIDE. The microbodies (Mb) maintain the same intimate relationship and orientation to the endoplasmic reticulum (ER) as shown in figure 21 but are extremely variable in size and shape and exhibit distortion and acute angulation of the marginal plates (arrow). M, mitochondrion. X 24,000

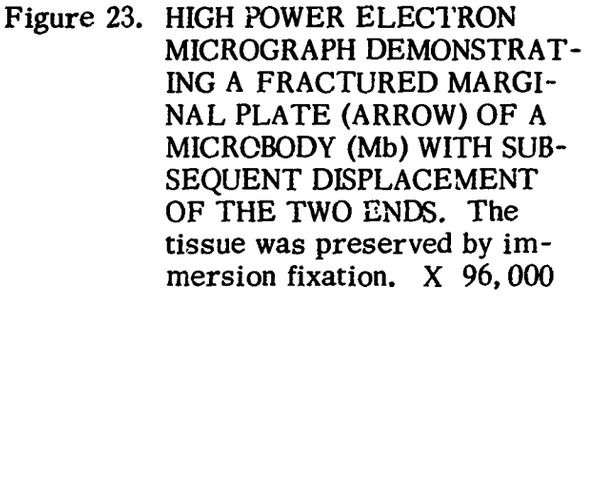

Figure 23. HIGH POWER ELECTRON MICROGRAPH DEMONSTRATING A FRACTURED MARGINAL PLATE (ARROW) OF A MICROBODY (Mb) WITH SUBSEQUENT DISPLACEMENT OF THE TWO ENDS. The tissue was preserved by immersion fixation. X 96,000

Two types of intramitochondrial inclusions are present in mitochondria of the rhesus monkey proximal tubule cells. The first type is composed of helical structures that lie entirely within widened cristae and are less electron dense than the surrounding mitochondrial matrix (figure 24). The inclusions are composed of filaments 30 to 40 angstroms in width. The diameter of the helix formed by the filaments is 130 to 140 angstroms with a pitch of approximately 120 angstroms. The coiled filaments usually run parallel to one another and often appear to twist or coil on each other. This was the most common type of mitochondrial inclusion observed in this material. Similar inclusions have been reported in mitochondria of astrocytes of the rat corpus striatum (Mugnaini, 1964) and within liver mitochondria following alcohol ingestion (Iseri et al, 1966; Porta et al, 1965). They have also been observed in hepatic cells of rats fed protein deficient diets (Svoboda and Higginson, 1964). The second type of inclusion lies free within the mitochondrial matrix and may represent a modification of the mitochondrial cristae (figure 25). It is composed of several parallel rows of membranes that resemble cristae. A regular periodicity of approximately 290 angstroms is present along these membranous profiles which appears to be the result of twisting of two of the parallel membranes to form a double helix. Additional details of this type of intramitochondrial inclusion can be found in reference 21. The significance of either of the two types of inclusions is not apparent but their presence in apparently normal non-diseased kidneys must be kept in mind when evaluating kidneys from experimental animals.

The thickness of the basement membrane of the proximal tubule in the rhesus monkey kidney decreases markedly from the first to the third segment. As shown on table I the average minimal thickness of the basement membrane of the first, second, and third segments is 2550 angstroms, 1460 angstroms and 703 angstroms, respectively. These findings emphasize the importance of identifying as precisely as possible the region of the proximal tubule under study in any investigation in which conclusions are being drawn regarding the significance of the thickness of the basement membrane and its possible relationship to a pathological condition. The thickness of the basement membrane also varies considerably depending upon the type of fixative and the method of fixation employed. As shown in table II, the basement membranes of proximal tubules fixed by immersion in osmiumt tetroxide have the greatest thickness, ranging from 1644 to 9799 angstroms. The mean values of the thinnest and thickest regions are 3578 ± 215 angstroms and 5692 ± 340 angstroms, respectively. In contrast, the mean values of the thinnest and thickest regions of the basement membrane of proximal tubules fixed by immersion in glutaraldehyde are 2569 ± 168 angstroms and 4280 ± 263 angstroms, respectively. As shown on table II, basement membrane thickness is nearly identical if proximal tubules are perfusion-fixed with osmium tetroxide or glutaraldehyde. Again, in any study in which conclusions are being drawn regarding the possible significance of the thickness of the basement membranes, the type of fixative employed and particularly the method of fixative application must be taken into consideration. A more detailed discussion of this problem can be found in reference 21.

TABLE I

COMPARISON OF BASEMENT MEMBRANE THICKNESS IN THREE SEGMENTS OF THE PROXIMAL TUBULE OF THE RHESUS MONKEY

Segment	No. of Measurements	Minimum thickness		Maximum thickness	
		Mean ± SEM (Å)	Range (Å)	Mean ± SEM (Å)	Range (Å)
First	56	2550* ± 107	1257-4470	3845* ± 154	2184-6515
Second	56	1460* ± 83	680-3333	2672* ± 137	1162-5833
Third	56	703 ± 28	363-1101	1523 ± 67	731-3252

* p = < 0.001 compared with third segment.

TABLE II

COMPARISON OF BASEMENT MEMBRANE THICKNESS OF THE FIRST SEGMENT OF THE PROXIMAL TUBULE FIXED IN GLUTARALDEHYDE AND OSMIUM TETROXIDE

Fixative	Method of Fixative Application	Minimum Thickness			Maximum Thickness		
		No. of Measure-ments	Mean, in Å (± S.E.M.)	Range, in Å	No. of Measure-ments	Mean, in Å (± S.E.M.)	Range, in Å
Glutaraldehyde	Immersion	28	2569 ±168	1302-4039	28	4280 ±263	2344-7374
Osmium Tetroxide	Immersion	28	3578* ±315	1644-7308	28	5092† ±340	2898-9799
Glutaraldehyde	IVIP‡	30	2518 ±154	1257-4258	30	4013 ±180	2204-6194
Osmium Tetroxide	IVIP‡	26	2588 ±153	1502-4470	26	3650 ±261	2184-6515

* P = 0.01
† P = 0.001
‡ in vivo intravascular perfusion

As discussed in an earlier section of this paper, the inner medulla of the kidney of the rhesus monkey is poorly developed. As a result, long loops of Henle, defined as those loops entering the inner medulla before forming the "hairpin" turn, are virtually absent. Thus, a long ascending thin limb segment is unusual. The overwhelming majority of the loops of Henle are short and do not enter the inner medulla. There is usually a very short descending thin limb segment but the "hairpin" turn is most often formed by tubular epithelium characteristic of the ascending thick limb of Henle (figure 26). The fine structural characteristics of the thin descending limb (figure 27) and the thick limb of Henle (figure 28) are nearly identical to other mammals including man. The typical thin limb cell is squamous in appearance and usually exhibits numerous short blunt microvilli on the apical or luminal cell surface. The cell bulges into the lumen in the region of the nucleus, but otherwise the cell cytoplasm is quite attentuated. Complicated lateral interdigitations exist between adjacent cells. Near the junction with the terminal proximal tubule, thin limb cells often contain large collections of lipofuscin or degeneration pigment (figure 29). Similar appearing collections of pigment have been noted in the human thin limb (Bulger et al, 1967). Cellular organelles are relatively sparse in this segment but qualitatively are identical to other segments of the nephron distal to the proximal tubule.

The epithelium of the thick limb of Henle is cuboidal and contains abundant quantities of mitochondria. The mitochondria are elongate and usually enclosed by plications of the basal plasmalemma (figure 28). The invaginations of the basal plasmalemma extend two-thirds of the distance toward the apical cell surface. Interdigitations of lateral and basilar cell processes between adjacent cells are complex and extensive. A prominent feature of this segment of the nephron is the presence of numerous small coated and non-coated apical vesicles located just beneath the apical plasmalemma (figure 30). The structure of this segment, in particular, the numerous mitochondria intimately associated with the basal plasmalemma correlates well with the active sodium transport capability known to be a functional characteristic of this segment of the nephron (Berliner and Bennett, 1967; Bennett et al, 1968).

After the thick ascending limb segment of the loop of Henle enters the cortical region, the tubule comes into contact with the same renal corpuscle from which the proximal tubule of that nephron originated. At the point of contact a specialized region of the distal tubule, the macula densa, is formed (figure 31). The most outstanding feature of this region is the change in polarity of the individual cells. The nucleus is apically-placed and the arrangement of organelles such as the Golgi apparatus, cytosomes, multivesicular bodies and cytosegresomes appears to be indicate of secretory or resorptive activity directed away from the lumen and toward the cell base as originally suggested by Goormaghtigh (1939). The appearance of the macula densa in the rhesus monkey is similar to other laboratory animals and man and will not be discussed in further detail. The macula densa along with granular myoepithelioid cells located in the wall of the terminal afferent arteriole and the lacis cells situated between the macula densa and the renal corpuscle form the juxtaglomerular apparatus (figure 32). Large "secretory" granules that probably represent renin or renin precursors are located within the myoepithelioid cells of the afferent arteriole and cells with features resembling both the myoepithelioid and lacis cells (figure 33). Similar granules are

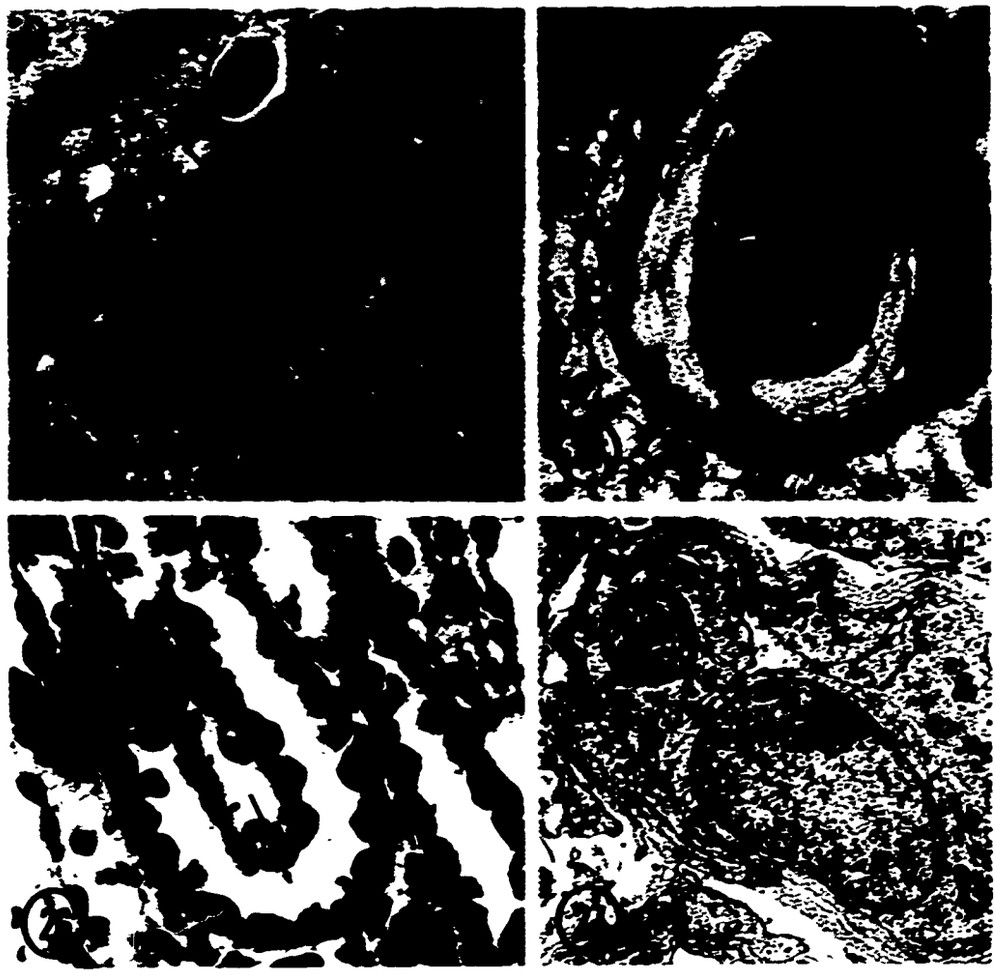

Figure 25. ELECTRON MICROGRAPH SHOWING A SECOND TYPE OF MITOCHONDRIAL INCLUSION (ARROW) WHICH IS MORE DENSE THAN SURROUNDING STRUCTURES AND COMPOSED OF SEVERAL PARALLEL ROWS OF MEMBRANES WHICH RESEMBLE MITOCHONDRIAL CRISTAE. See text for description. X 13,800

Figure 24. ELECTRON MICROGRAPH SHOWING MITOCHONDRIAL INCLUSION (ARROW) LYING ENTIRELY WITHIN A WIDENED CRISTAE. See text for description. X 47,400

Figure 26. PHOTOMICROGRAPH FROM THE OUTER MEDULLA DEMONSTRATING A "HAIRPIN" TURN (ARROW) OF THE LOOP OF HENLE FORMED ENTIRELY BY EPITHELIUM CHARACTERISTIC OF THE THICK SEGMENT. Cells are cuboidal and contain large numbers of mitochondria and other cellular organelles. Gomori trichrome stain. X 640

Figure 27. ELECTRON MICROGRAPH SHOWING THE APPEARANCE OF A THIN DESCENDING LIMB SEGMENT IN THE OUTER MEDULLA. Lining cells are simple squamous in type and contain few mitochondria or other organelles. Small blunt microvilli are numerous on the luminal cell surface (arrow). BM, basement membrane; IC, interstitial cell with lipid inclusion. X 4600

not observed within lacis cells, cells of the macula densa, or the efferent arteriole. Both circular homogenous electron-dense cytosomes and cytosomes containing oblong "granules" measuring up to 6 microns in length (figure 34) are seen. The oblong structures contain a central dense core with a highly ordered crystalline structure exhibiting a regular periodicity of approximately 80 angstroms. The central core is surrounded in most instances by a less dense homogeneous matrix.

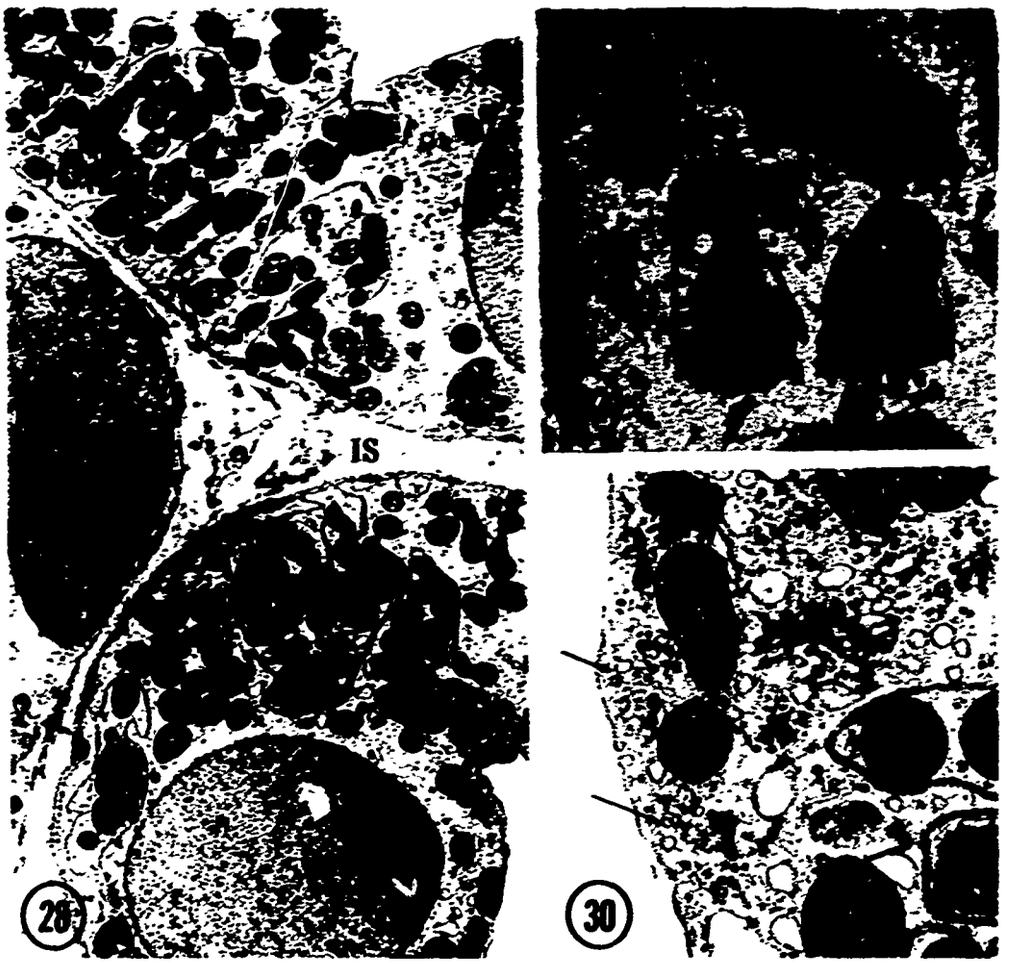

Figure 28. ELECTRON MICROGRAPH OF THICK LIMB SEGMENTS IN THE OUTER MEDULLA. The cells are cuboidal and contain numerous mitochondria (M), many of which are in intimate association with invaginations of the basal plasmalemma. IS, interstitial space. X 4500

Figure 29. ELECTRON MICROGRAPH SHOWING LARGE COLLECTIONS OF LIPOFUSCIN OR DEGENERATION PIGMENT IN THIN LIMB SEGMENTS OF THE RHESUS MONKEY KIDNEY. X 16,450

Figure 30. ELECTRON MICROGRAPH SHOWING THE NUMEROUS VESICLES (ARROWS) IN THE APICAL REGION OF A CELL TYPICAL OF THE ASCENDING THICK LIMB OF HENLE. GA, Golgi apparatus. X 12,800

Figure 31. ELECTRON MICROGRAPH SHOWING THE STRUCTURE OF TYPICAL MACULA DENSA CELLS. The nuclei (N) are apically-placed and other cellular organelles including the Golgi apparatus (GA), cytosomes (C), and multivesicular bodies (MvB) are located toward the basal surface of the cell suggesting a reversed functional polarity. See text for possible functional significance. L, lumen of tubule. X 4, 000

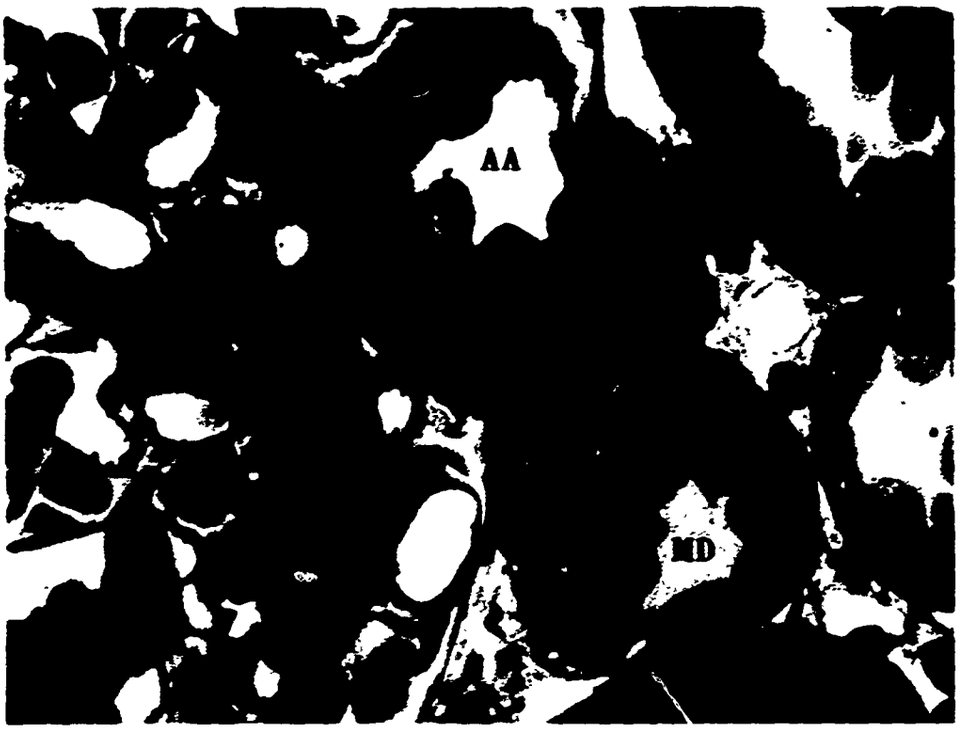

Figure 32. PHOTOMICROGRAPH SHOWING THE TYPICAL APPEARANCE OF A JUXTA-GLOMERULAR APPARATUS WHICH INCLUDES THE MACULA DENSA (MD), THE AFFERENT ARTERIOLE (AA) AND THE LACIS CELLS (LC) IN THE REGION OF THE POLKISSEN. X 525

Figure 33. ELECTRON MICROGRAPH OF PORTIONS OF A JUXTA-GLOMERULAR APPARATUS SHOWING THE AFFERENT ARTERIOLE (AA) AT THE UPPER RIGHT AND THE MACULA DENSA (MD) AT THE LOWER RIGHT. Numerous dense secretory granules are present within myoepithelioid and other contiguous cells. X 4,500

The distal convoluted tubule, extending from the macula densa to the connecting segment of the cortical collecting tubule, is similar in structure to the ascending thick limb of Henle. The cells are cuboidal to low columnar and easily identified by their large complement of elongate mitochondria enclosed within plications of the basal plasmalemma (figures 35 and 36). Dark or intercalated cells which have recently been described in the distal convoluted tubule of the rat (Griffith et al, 1968) and man (Tisher et al, 1968) are also present within the distal convoluted tubule of the rhesus monkey kidney (Tisher, unpublished observations). There is a gradual transition from the distal convoluted tubule to the cortical collecting duct.

Figure 34. HIGH MAGNIFICATION ELECTRON MICROGRAPH OF A MYOEPITHELIOID CELL CONTAINING THE RECTANGULAR OR OBLONG SECRETORY GRANULES BELIEVED TO BE RENIN. Many granules have a central density with a crystalline substructure of approximately 80 angstrom periodicity surrounded by less dense material. X 27, 800

Figure 35. PHOTOMICROGRAPH OF DISTAL CONVOLUTED TUBULES (DT) FROM RHESUS MONKEY KIDNEY. X 600

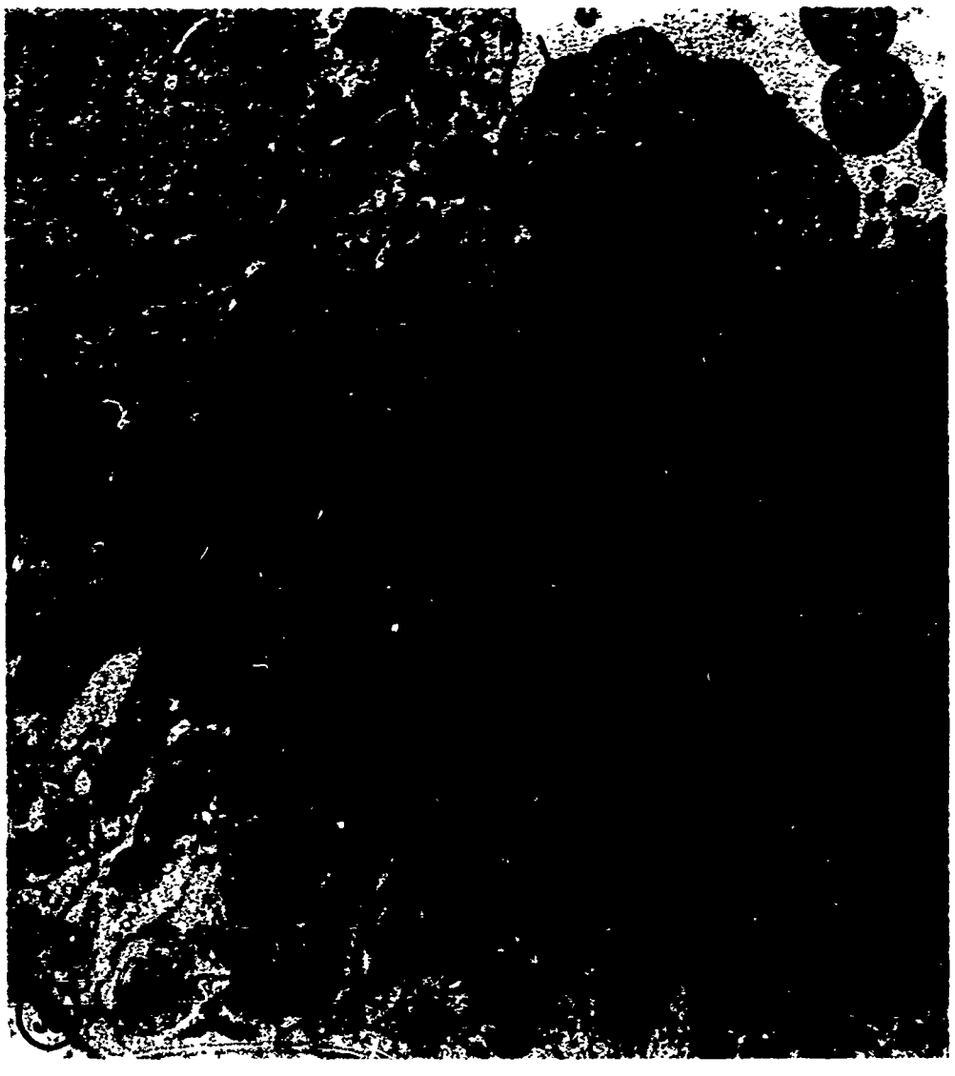

Figure 36. ELECTRON MICROGRAPH OF A DISTAL CONVOLUTED TUBULE. The cells are filled with elongate mitochondria (M), many enclosed within plications of the basal plasmalemma. Numerous vesicles are apparent on the apical cell surface (arrow). X 9,000

For purposes of organization, the collecting duct can be divided into four segments based primarily on their location in the kidney. The initial segment, the cortical collecting tubule or connecting segment, extends from its transition with the distal convoluted tubule to the medullary ray. The three remaining segments include the collecting tubule in the medullary ray, the outer medullary segment, and the inner medullary segment. With the exception of the inner medullary segment, the structural characteristics of the collecting duct of the rhesus monkey are nearly identical to that of the human kidney. The inner medullary segment is extremely abbreviated in length, however, compared to man. As the collecting ducts of the outer medulla descend toward the inner medulla they join very quickly to form the ducts of Bellini. These ducts are lined by a modified type of transitional epithelium, identical in appearance to the epithelium overlying the tip of the renal papilla (Tisher, in press) (figure 37). The collecting duct or tubule contains two types of cells, the light cell which is the principal cell type and the "intercalated" or dark cell (figure 38). The latter are most abundant in the cortical collecting tubule and decrease in frequency as the collecting duct descends into the inner medulla. In the inner medulla only light cells are present. The light cells contain a rather clear cytoplasm, a centrally-placed nucleus, and small numbers of randomly oriented mitochondria (figure 39). The dark cells possess a much darker cytoplasm due to the presence of increased numbers of cellular organelles including mitochondria, lysosomes, and granulated endoplasmic reticulum (figure 40). As in the human, the individual cells of the collecting duct progressively increase in height as the duct descends into the inner medullary region. With the exception of the inner medullary segment, the fine structural characteristics of the rhesus monkey collecting duct closely parallel those of man.

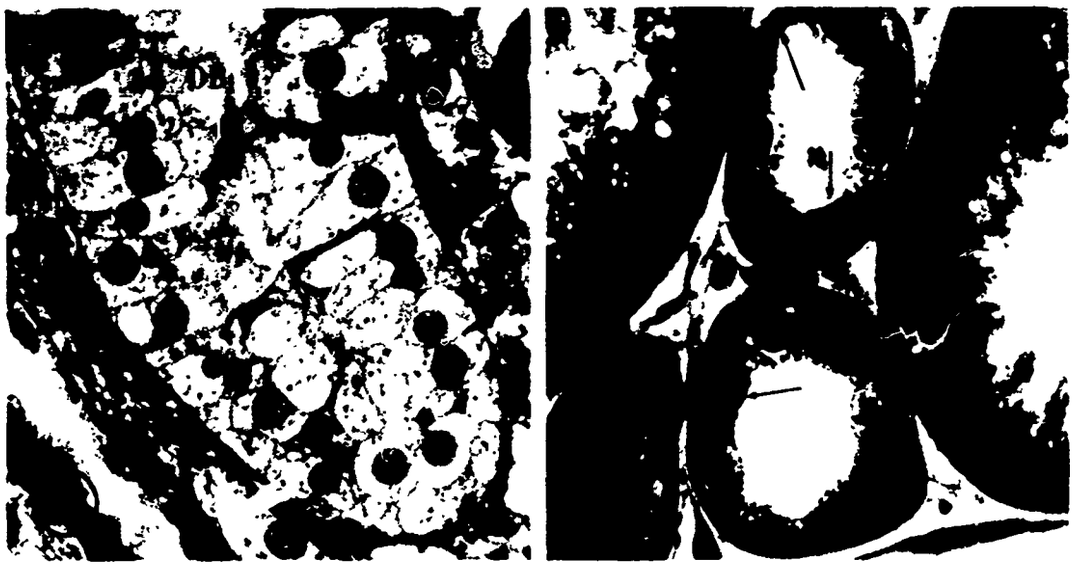

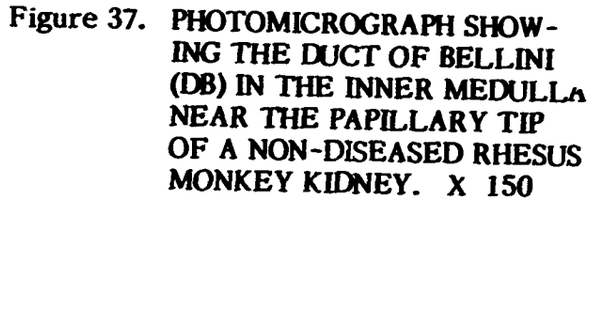

Figure 37. PHOTOMICROGRAPH SHOWING THE DUCT OF BELLINI (DB) IN THE INNER MEDULLA NEAR THE PAPILLARY TIP OF A NON-DISEASED RHESUS MONKEY KIDNEY. X 150

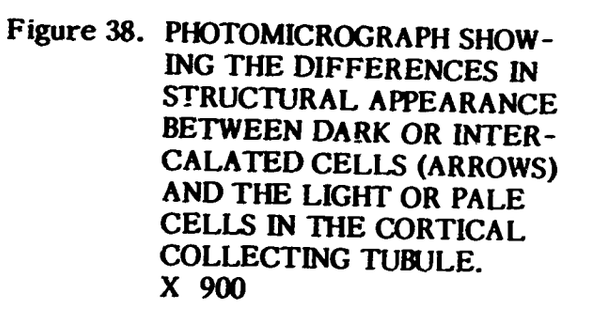

Figure 38. PHOTOMICROGRAPH SHOWING THE DIFFERENCES IN STRUCTURAL APPEARANCE BETWEEN DARK OR INTERCALATED CELLS (ARROWS) AND THE LIGHT OR PALE CELLS IN THE CORTICAL COLLECTING TUBULE. X 900

Figure 39. AN ELECTRON MICROGRAPH SHOWING THE TYPICAL APPEARANCE OF LIGHT OR PALE CELLS IN THE CORTICAL COLLECTING TUBULE. Note the paucity of organelles and the random distribution of mitochondria throughout the cell cytoplasm. X 15, 750

Figure 40. ELECTRON MICROGRAPH OF A DARK OR INTERCALATED CELL FROM THE CORTICAL COLLECTING TUBULE. The cytoplasm is very dense and contains large numbers of free ribosomes and clusters of rough surfaced endoplasmic reticulum, cytosomes, and increased numbers of mitochondria. Small microvilli are present on the apical surface of the cell (arrow). The basal plasmalemma is much more complex in configuration than that of light cells within this segment of the nephron. PC, peritubular capillary. X 9, 240

In summary, gross, light and electron microscopic morphological observations of the kidney of the non-diseased rhesus monkey ~~have been~~ presented. Where pertinent, certain parameters of renal function ~~have been~~ reviewed and appropriate correlations made with the structure of the kidney. At the ultrastructural level, emphasis ~~has been~~ placed on many morphological variations in the kidney that have been observed in these apparently non-diseased animals. In part, these variations appear to represent biological differences among individual animals exposed to a "hostile" environment. Finally, morphological variations that can be ascribed to the method of tissue preservation that has been employed ~~have been~~ stressed.

ACKNOWLEDGEMENTS

The author gratefully acknowledges the valuable contributions of several colleagues involved in various aspects of the work reported in the present paper. These individuals include Drs. Seymour Rosen, Richard M. Finkel, Paul E. Teschan, and R.W. Schrier. Permission was granted by the editors of the American Journal of Pathology to reproduce figures 11-20, 23-25, and 29, and tables I and II from a previous publication by the author (Tisher et al, 1969). Similar permission was granted by the editors of Laboratory Investigation to reproduce figures 6, 8, 10, 21, 22, and 33 from previous publications by the author (Rosen and Tisher, 1968; Tisher et al, 1968). Figures 31 and 36 were kindly supplied by Dr. Seymour Rosen to whom the author is greatly indebted.

REFERENCES

1. Bennet, C.M., B.M. Brenner and R.W. Berliner; "Micropuncture Study of Nephron Function in the Rhesus Monkey"; J. Clin. Invest., 47:203-216, 1968.

2. Berliner, R.W. and C.M. Bennett; "Concentration of Urine in the Mammalian Kidney"; Amer. J. Med., 42: 777-789, 1967.

3. Bulger, R.E., C.C. Tisher, C.H. Myers and B.F. Trump; "Human Renal Ultrastructure. II. The Thin Limb of Henle's Loop and the Interstitium in Healthy Individuals"; Lab. Invest., 16:124-141, 1967.

4. De Martino, C., L. Accini, G.A. Andres and I. Archetti; "Tubular Structures Associated with the Endothelial Endoplasmic Reticulum in Glomerular Capillaries of Rhesus Monkey and Nephritic Man"; Z. Zellforsch., 97:502-511, 1969.

5. Goormaghtigh, N.; "Existence of an Endocrine Gland in the Media of Renal Arterioles"; Proc. Soc. Exp. Biol. Med., 42:688-689, 1939.

6. Griffith, L.D., R.E. Bulger and B.F. Trump; "Fine Structure and Staining of Mucosubstances on 'Intercalated Cells' from the Rat Distal Convoluted Tubule and Collecting Duct"; Anat. Rec., 160:643-661, 1968.

REFERENCES (Cont'd)

7. Iseri, O.A., C.S. Lieber and L.S. Gottlieb; "The Ultrastructure of Fatty Liver Induced by Prolonged Ethanol Ingestion"; Am. J. Path., 48:535-555, 1966.

8. Jorgensen, F. and M.W. Bentzon; "The Ultrastructure of the Normal Human Glomerulus. Thickness of Glomerular Basement Membrane"; Lab. Invest., 18:42-48, 1968.

9. Kanamitsu, M., A. Kasamaki, M. Ogawa, S. Kasahara and M. Imamura; "Immunofluorescent Study on the Pathogenesis of Oral Infection of Poliovirus in Monkey"; Jap. J. Med. Sci. Biol, 20:175-194, 1967.

10. Kim, K.S.W. and E.S. Boatman; "Electron Microscopy of Monkey Kidney Cell Cultures Infected with Rubella Virus"; J. Virol., 1:205-214, 1967.

11. Mugnaini, E.; "Helical Filaments in Astrocytic Mitochondria of the Corpus Striatum in the Rat"; J. Cell. Biol., 23:173-182, 1964.

12. Porta, E.A., W.S. Hortroft and F.A. De La Iglesia; "Hepatic Changes Associated with Chronic Alcoholism in Rats"; Lab. Invest., 14:1437-1455, 1965.

13. Rosen, S. and C.C. Tisher; "Observations on the Rhesus Monkey Glomerulus and Juxtaglomerular Apparatus"; Lab. Invest., 18:240-248, 1968.

14. Strunk, S.W., W.S. Hammond and E.P. Benditt; "The Resolution of Acute Glomerulonephritis. An Electron Microscopic Study of Four Sequential Biopsies"; Lab. Invest., 13:401-429, 1964.

15. Svoboda, D.J. and J. Higginson; "Ultrastructural Changes Induced by Protein and Related Deficiencies in the Rat Liver"; Am. J. Path., 45:353-380, 1964.

16. Tisher, C.C., R.E. Bulger and B.F. Trump; "Human Renal Ultrastructure. I. Proximal Tubules of Healthy Individuals"; Lab. Invest., 15:1357-1394, 1966.

17. Tisher, C.C. and S. Rosen; "Ultrastructure of Renal Proximal Tubules of the Rhesus Monkey: A Comparison with the Human"; Lab. Invest., 16:637, 1967.

18. Tisher, C.C., S. Rosen and P. Teschan; "Morphology of Henle's Loop and Its Relation to Urinary Concentrating Ability in Monkey and Man"; Fed. Proc., 27: 741, 1968.

19. Tisher, C.C., R.E. Bulger and B.F. Trump; "Human Renal Ultrastructure. III. The Distal Tubule in Healthy Individuals"; Lab. Invest., 18:655-668, 1968.

20. Tisher, C.C., R.M. Finkel, S. Rosen and E.M. Kendig; "Renal Microbodies in the Rhesus Monkey"; Lab. Invest., 19:1-6, 1968.

REFERENCES (Cont'd)

21. Tisher, C.C., S. Rosen and G.B. Osborne; "Ultrastructure of the Proximal Tubule of the Rhesus Monkey Kidney"; Am. J. Path., 56:469-517, 1969.

22. Tisher, C.C., R. Ranney, J.S. McNeil and R.W. Schrier; "Evaluation of Concentrating Ability and Renal Morphology in the Macaque Monkey: Finding of Pitressin-Resistant Hyposthenuria"; Clin. Res., 18:66, 1970.

23. Tisher, C.C.; "Relationship Between Renal Structure and Concentrating Ability in the Rhesus Monkey". (Manuscript submitted for publication).

24. Tisher, C.C. Unpublished Observations.

DISCUSSION

DR. BEARD: Dr. Tisher, I'm greatly impressed with the beauty of your pictures. I'm not a pathologist, I don't know too much about this but one point which I hope you'll bring out in publishing this is what you mean by healthy and normal. I presume these animals had their share of intestinal parasites.

DR. TISHER: Yes, that certainly is true, but by the clinical tests that are commonly employed, with particular stress on renal function tests, these animals were not clinically diseased. To give you an example, we measured electrolytes repeatedly, looked at urinary sediment, measured the endogenous creatinine clearances, and they also had a full battery of liver enzymes. We recognized the fact that they could have intestinal parasites. They were routinely checked and when this was confirmed, they were treated.

DR. PECK (Merck Institute for Therapeutic Research): I greatly appreciate the information you've presented. This is one of our problems in the area of drug toxicity, what is the change due to the drug and the change due to normal physiological conditions, diuresis, or increased blood flow. How can we interpret these changes as being something which is pathological or something which is physiological. We need more publications like this to help us along.